

ASYMPTOTICS OF A SLOW MANIFOLD

J. VANNESTE*

Abstract. Approximately invariant elliptic slow manifolds are constructed for the Lorenz–Krishnamurthy model of fast–slow interactions in the atmosphere. As is the case for many other two-time-scale systems, the various asymptotic procedures that may be used for this construction diverge, and there are no exactly invariant slow manifolds. Valuable information can however be gained by capturing the details of the divergence: this makes it possible to define exponentially accurate slow manifolds, identify one of these as optimal, and predict the amplitude and phase of the fast oscillations that appear for trajectories started on it. We demonstrate this for the Lorenz–Krishnamurthy model by studying the slow manifolds obtained using a power-series expansion procedure. We develop two distinct methods to derive the leading-order asymptotics of the late coefficients in this expansion. Borel summation is then used to define a unique slow manifold, regarded as optimal, which is piecewise analytic in the slow variables. This slow manifold is not analytic on a Stokes surface: when slow solutions cross this surface, they switch on exponentially small fast oscillations through a Stokes phenomenon. We show that the form of these oscillations can be recovered from the Borel summation. The approach that we develop for the Lorenz–Krishnamurthy model has a general applicability; we sketch how it generalises to a broad class of two-time scale systems.

Key words. Slow manifold, exponential asymptotics, atmospheric waves

AMS subject classifications. 37N10, 76B15, 76U05, 37K05

1. Introduction. Dynamical systems with two time scales appear in a wide variety of applications, in physics and chemistry in particular. A central concept in their analysis is that of slow manifold [28, 18, 19]. Slow manifolds are nearly invariant submanifolds of the state space of these systems near which the dynamics is slow; their dimension is the number of slow variables, and they are defined by constraints slaving fast variables to slow ones (see, e.g., [25]). The advantages of identifying slow manifolds in two time-scale systems are obvious: projecting the dynamics onto a slow manifold leads to a dynamical system of reduced dimensionality; this system approximates the full dynamics while filtering out the fast behaviour, and it can therefore be integrated efficiently.

The fast behaviour we are concerned with in this paper consists of rapid undamped oscillations. In this case, the slow manifolds are elliptic and hence fragile. Specifically, if $\epsilon \ll 1$ is the small parameter characterising the separation between fast and slow time scales, the slow manifold that exists for $\epsilon = 0$ cannot be expected to persist as an invariant object when $\epsilon \neq 0$. This is of course in contrast with the normally hyperbolic case, for which persistence can be established [13]. Even though elliptic slow manifolds are generally not exactly invariant, they can be approximately so to a very high degree of accuracy. Indeed, systematic asymptotic procedures make it possible to improve this accuracy, estimated by the angle between the vector field and the manifold, systematically order-by-order in ϵ . For analytic vector fields, it is possible to construct slow manifolds with $O(\epsilon^n)$ accuracy for arbitrary $n \in \mathbb{N}$ and even, by optimal truncation, to achieve exponential accuracy [15, 11, 35, 25, 12, 27].

The non-existence of exactly invariant slow manifolds reflects the fact that fast activity cannot be completely filtered out by a suitable projection of the initial conditions. In other words, in the elliptic situation, fast oscillations are typically generated by the slow dynamics, however well the initial data are prepared. The non-invariance

*School of Mathematics and Maxwell Institute, University of Edinburgh, King’s Buildings, Edinburgh EH9 3JZ, UK (J.Vanneste@ed.ac.uk).

is also manifested by the divergence of the asymptotic procedures used in the construction of slow manifolds. The two aspects are related: the nature of the divergence — the manner in which the coefficients of ϵ^n in the power-series expansions defining slow manifolds grow with n — encodes the generation of (exponentially small) oscillations. Thus, capturing the details of the divergence provides a means of describing these oscillations. It also gives a way of analysing the differences between the various slow manifolds that are obtained near optimal truncation. One of the motivations here is to distinguish, among these slow manifolds differing by exponentially small terms, a unique one, enjoying special properties.

The exponential accuracy of elliptic slow manifolds, the divergence of the asymptotic procedures used in their construction, and the connection between this divergence and the generation of fast oscillations are the themes of this paper. Although these have a general appeal for a broad class of two time-scale systems, we mainly explore them in a specific context, and for a specific model. The context is geophysical fluid dynamics. Because of the fast rotation of the earth, the mid-latitude atmosphere and oceans are typical two-time-scale systems, with the corresponding small parameter — the Rossby number — taking values of the order of 0.1 and 0.01 in the atmosphere and the oceans, respectively. Furthermore, the nature of the forcing is such that the fast degrees of freedom, consisting of inertia-gravity waves, are often only weakly excited. As a result, the notion of slow manifold is eminently relevant. (See, e.g., [34, 31] and references therein for more background.)

The specific model that we analyse is the Lorenz five-component model [21], often referred to as the Lorenz–Krishnamurthy (LK) model [23]. This model, governed by five ordinary differential equations, was devised by Lorenz in order to explore the concept of slow manifolds and study their invariance. Since it was proposed, it has become one of the main testbeds for the study of slow manifolds, reduced models (termed balanced models in this context), spontaneous wave generation, etc. in geophysical fluid dynamics [21, 22, 23, 9, 10, 14, 32, 6, 7, 8, 17, 29, 30].

Several asymptotic procedures have been proposed for the derivation of slow manifolds in the LK models (e.g. [20, 32]). Since their divergence properties are identical, we concentrate here on a particularly simple one (see [34] for a detailed discussion). Specifically, a slaving relation, which defines the slow manifold by relating the fast variables to the slow ones, is postulated and introduced into the dynamical equations. An approximate solution of the resulting partial differential equation is then sought as a series expansion in powers of the small parameter ϵ . The coefficients in this series, which we term slaving coefficients, are functions of the slow variables. Our main aim is to capture their late form, that is, to obtain the asymptotics of the coefficient of ϵ^n as $n \rightarrow \infty$. Two alternative approaches are discussed. These are interchangeable in the case of the LK model, but one or the other may be preferable for more complicated models. Remarkably, the leading-order asymptotics of the slaving coefficients can be determined in closed form, up to a single constant which is readily estimated by solving a recurrence relation numerically. The accuracy of the asymptotic result is established by a comparison with the slaving coefficients computed numerically for a range of values of the slow variables.

We emphasise that our asymptotic results give a precise description of the manner with which the power series expansion defining the slow manifolds diverges as $n \rightarrow \infty$. This makes it possible to go beyond the standard optimal truncation arguments (e.g. [11, 35]), which only provide bounds on the accuracy of the slow manifold, and delve into the dynamics of the exponentially small terms. Specifically, we use the Borel

summation of the divergent power series [3, 2] to define a unique manifold, which we term optimal slow manifold. This is defined in a piecewise manner, with discontinuities across codimension-one surfaces. Trajectories started on the optimal slow manifold move away from it by an exponentially small distance when they cross these surfaces, and fast oscillations develop. The amplitude and phase of these oscillations can be determined from the late behaviour of the slaving coefficients. In previous work [29], we derived these amplitude and phase by considering the dynamics along specific trajectories. The present approach recovers these results by taking a more geometric perspective, which views the slow manifold as a single object rather than a collection of slow trajectories.

The analysis we carry out for the LK model is representative of a more general treatment applicable to more complicated two-time-scale systems. We make this plain by also considering a broad class of such systems and sketching how the theory developed for the LK model generalises to this class. The results presented are largely formal, and they make a number of simplifying assumptions, in particular about the nature of the singularities of slow trajectories in the complex time plane. Nevertheless, they provide a first glimpse into the relationship between these singularities, the divergence of the asymptotic procedures used for constructing slow manifolds, and the generation of fast oscillations.

This paper is organised as follows. The LK model is introduced in section 2. There we discuss a systematic approach for the construction of slow manifolds of increasing accuracy. As mentioned, this approach relies on expanding in power series of ϵ the relations which define the slow manifolds by slaving fast variables to slow variables. The coefficients of ϵ^n in this expansion — the slaving coefficients — satisfy recurrence relations involving partial derivatives with respect to the slow variables. The nonlinearity of the LK model, involving only quadratic terms, is simple enough that the slaving coefficients are homogeneous polynomials in the slow variables. It is therefore easy to derive them by solving simple algebraic recurrences for the coefficients of these polynomials. Section 3 focuses on these coefficients, which we refer to as polynomial coefficients to distinguish them from the slaving coefficients. Specifically, we examine the form of the polynomial coefficients for large n . Two asymptotic results are obtained. The first result gives a Gaussian approximation to the slaving coefficients. The second, more general, result improves on this approximation in the same manner as the large-deviation theory for the probability density of sums of random numbers improves on the central-limit theorem. Section 4 then considers the large- n asymptotics of the slaving coefficients themselves. The asymptotic behaviour is obtained using two different approaches, one based on the polynomial coefficients, the other directly considering the partial differential equation satisfied by the slaving coefficients. The results are exploited in section 5, where we discuss the resummation of the divergent series defining the slow manifolds. There, we use Borel summation (e.g. [3, 2]) to define a unique slow manifold which we regard as optimal. The slaving relation for this slow manifold is given as an integral which is clearly discontinuous across certain surfaces in the slow space. Examining the dynamics across these surfaces, we demonstrate that it is characterised by the generation of exponentially small fast oscillations whose form is encoded in the Borel sum. General two-time-scale systems with elliptic slow manifolds are considered in section 6. The paper concludes with a discussion in section 7.

2. Formulation.

2.1. Model. We consider the model devised by Lorenz [21] and variously referred to as the Lorenz five-component model or as the Lorenz–Krishnamurthy model (LK, [23]). In its conservative form, on which we will focus, it can be written as the set of five ordinary differential equations

$$(2.1) \quad \dot{u} = -vw + \epsilon bvy,$$

$$(2.2) \quad \dot{v} = uw - \epsilon buy,$$

$$(2.3) \quad \dot{w} = -uv,$$

$$(2.4) \quad \epsilon \dot{x} = -y,$$

$$(2.5) \quad \epsilon \dot{y} = x + buv,$$

for the five dependent variables (u, v, w, x, y) . This model, obtained by truncation of the rotating shallow-water equations, governs the dynamics of a triad of vortical modes, with amplitudes (u, v, w) , coupled to a gravity mode described by (x, y) . The two parameters b and ϵ of the model control the strength of the coupling and the gravity-wave frequency, respectively.

Following Camassa [9] and Bokhove and Shepherd [6], we note that the constancy of the $u^2 + v^2$, obvious from (2.1)–(2.2), can be used to reduce the dimension of the LK model from 5 to 4. Specifically, letting

$$(2.6) \quad u = u_0 \cos \phi \quad \text{and} \quad v = u_0 \sin \phi,$$

reduces (2.1)–(2.5) to the two degree-of-freedom Hamiltonian system

$$(2.7) \quad \dot{\phi} = w - \epsilon by$$

$$(2.8) \quad \dot{w} = -u_0^2 \sin(2\phi)/2$$

$$(2.9) \quad \epsilon \dot{x} = -y,$$

$$(2.10) \quad \epsilon \dot{y} = x + bu_0^2 \sin(2\phi)/2.$$

Here, $u_0^2 = u^2 + v^2$ is a constant which could be set to 1 by scaling.

In the form (2.7)–(2.10), the LK model can be recognised as describing the dynamics of a pendulum (making an angle 2ϕ with the vertical), coupled in some way to a spring of extension x . This interpretation is useful to develop some intuition about the dynamics of the model; it also makes transparent the relationship between the LK model and mechanical models such as the swinging spring (or elastic pendulum; see, e.g., [24]). In what follows, we mostly use the original formulation (2.1)–(2.5), which gives a more compact form to various mathematical expressions; however, we often use the variable ϕ in place of (u, v) to display functions of (u, v, w) in the reduced, two-dimensional space (ϕ, w) .

We are interested in the dynamics of the LK model when $\epsilon \ll 1$. In this regime, there is a large separation between the $O(1)$ time scale of evolution of the slow variables (u, v, w) and the $O(\epsilon)$ time scale of the fast variables (x, y) . We also assume that $b = O(1)$. In the geophysical context, these assumptions correspond to the quasi-geostrophic regime, in which fast gravity waves interact only weakly with the much slower vortical motion, termed balanced motion. In the mechanical interpretation of the LK model, $\epsilon \ll 1$ indicates that the spring is stiff, so that its frequency ϵ^{-1} far exceeds that of the pendulum.

The large time-scale separation implies the existence of slow manifolds. For the LK model, these are three-dimensional submanifolds of the state space, parameterized

by (u, v, w) , which are nearly invariant and near which the motion is slow. The dynamics in the neighbourhood of such slow manifolds is approximately devoid of the fast oscillations which characterise the dynamics elsewhere in the state space. The slow manifolds are elliptic, since linearising the fast dynamics gives the purely imaginary eigenvalues $\pm i\epsilon^{-1}$. Therefore they cannot be expected to be invariant when $\epsilon \neq 0$. Nevertheless, their accuracy, measured by the difference between the angle made by the vector field $(\dot{u}, \dot{v}, \dot{w}, \dot{x}, \dot{y})$ and the slow manifold, can be very high indeed: systematic improvement procedures make it possible to define slow manifolds with exponentially small errors.

The main interest of slow manifolds is that they allow a simplified description of the dynamics. Projecting the vector field onto a slow manifold leads to a reduced system of slow equations for (u, v, w) which approximates well the full dynamics for initial condition near the slow manifold. Reduced models obtained in this manner are termed balanced models in the geophysical context, where they have proved highly successful.

It is clear from (2.4)–(2.5) that a slow manifold for the LK model can be defined as the graph

$$(2.11) \quad x = -buv \quad \text{and} \quad y = 0.$$

The corresponding balanced model is then given by (2.1)–(2.3) with $y = 0$. The slow manifold (2.11) is only a leading-order approximation; starting with Lorenz [21], many authors have considered how this can be improved. In the next sections, we examine in detail a simple asymptotic procedure of the type described by Warn et al. [34] which leads to an arbitrary $O(\epsilon^n)$ accuracy. Our aim is to capture the manner in which this procedure diverges so as to define a slow manifold with a better-than-exponential accuracy.

2.2. Slow manifolds. Slow manifolds can be sought by introducing the so-called slaving relations

$$(2.12) \quad x = X(u, v, w; \epsilon) \quad \text{and} \quad y = Y(u, v, w; \epsilon),$$

for unknown functions X and Y into (2.4)–(2.5). Eliminating the time derivatives by means of (2.1)–(2.3) gives what Lorenz [20] termed the ‘superbalance equation’, namely

$$(2.13) \quad \epsilon \left[\frac{\partial X}{\partial u}(-vw + \epsilon bvy) + \frac{\partial X}{\partial v}(uw - \epsilon buy) - \frac{\partial X}{\partial w}uv \right] = -Y,$$

$$(2.14) \quad \epsilon \left[\frac{\partial Y}{\partial u}(-vw + \epsilon bvy) + \frac{\partial Y}{\partial v}(uw - \epsilon buy) - \frac{\partial Y}{\partial w}uv \right] = X + buv.$$

These are two coupled partial differential equations for X and Y for which approximate solutions can be found using iteration or expansion in powers of ϵ . Here we employ the latter method which is more suited to derive explicit results. To some extent the method used is irrelevant, since the slow manifolds obtained by different means coincide up to terms smaller than the accuracy of the methods. Nevertheless, specific methods may have some advantage: for instance, the iterative procedure proposed in [25] guarantees that all equilibria of the system near the slow manifold lie exactly on it. The expansion used here does not have this property.

Inspection of (2.13)–(2.14) indicates that power series expansions of the slaving relations (2.12) take the form

$$(2.15) \quad x = \sum_{n=0}^N \epsilon^{2n} X_n(u, v, w) \quad \text{and} \quad y = \sum_{n=0}^N \epsilon^{2n+1} Y_n(u, v, w),$$

where the functions of the slow variables X_n and Y_n are termed slaving coefficients. These are homogenous polynomials in u , v and w of degree $2n + 2$ and $2n + 3$, respectively. We make their specific form explicit by writing

$$(2.16) \quad X_n(u, v, w) = (2n)! \sum_{i,j=0} C_{ij}^n u^{2i+1} v^{2j+1} w^{2k},$$

with $k = n - i - j \geq 0$, and

$$(2.17) \quad Y_n(u, v, w) = (2n + 1)! \sum_{i,j=0} D_{ij}^n u^{2i} v^{2j} w^{2k+1},$$

with $k = n + 1 - i - j \geq 0$. In defining the coefficients C_{ij}^n and D_{ij}^n , we have introduced the normalization factors $(2n)!$ and $(2n + 1)!$ which roughly capture the dominant growth of X_n and Y_n with n . We refer to C_{ij}^n and D_{ij}^n as polynomial coefficients and emphasise that, unlike the slaving coefficients X_n and Y_n which they generate, they are simply numbers (for fixed b).

Substituting (2.15)–(2.17) into (2.13)–(2.14) leads to the following recurrence relations for the C_{ij}^n and D_{ij}^n :

$$(2.18) \quad \begin{aligned} (2n + 1)D_{ij}^n &= (2i + 1)C_{i(j-1)}^n - (2j + 1)C_{(i-1)j}^n + (2k + 2)C_{(i-1)(j-1)}^n \\ &- b \sum_{m=0}^{n-1} \sum_{p,q=0}^m \frac{(2m)!(2n - 2m - 1)!}{(2n)!} C_{pq}^m \\ &\times \left[(2p + 1)D_{(i-p)(j-q-1)}^{n-m-1} - (2q + 1)D_{(i-p-1)(j-q)}^{n-m-1} \right], \end{aligned}$$

where $k = n + 1 - i - j$, and

$$(2.19) \quad \begin{aligned} 2nC_{ij}^n &= -2(i + 1)D_{(i+1)j}^{n-1} + 2(j + 1)D_{i(j+1)}^{n-1} - (2k + 1)D_{ij}^{n-1} \\ &+ b \sum_{m=0}^{n-2} \sum_{p,q=0}^{m+1} \frac{(2m + 1)!(2n - 2m - 3)!}{(2n - 1)!} D_{pq}^m \\ &\times \left[2pD_{(i-p+1)(j-q)}^{n-m-2} - 2qD_{(i-p)(j-q+1)}^{n-m-2} \right], \end{aligned}$$

where $k = n - i - j$. The initial condition for this iteration is provided by the leading-order slow manifold (2.11) which gives

$$(2.20) \quad C_{00}^0 = -b.$$

The successive D_{ij}^n and C_{ij}^n are then calculated from (2.18)–(2.19), with the convention that $D_{ij}^n = 0$ for $i < 0$, $j < 0$ or $i + j > n + 1$, and $C_{ij}^n = 0$ for $i < 0$, $j < 0$ or $i + j > n$. The first few coefficients are

$$(2.21) \quad D_{00}^0 = 0, \quad D_{10}^0 = b, \quad D_{01}^0 = -b,$$

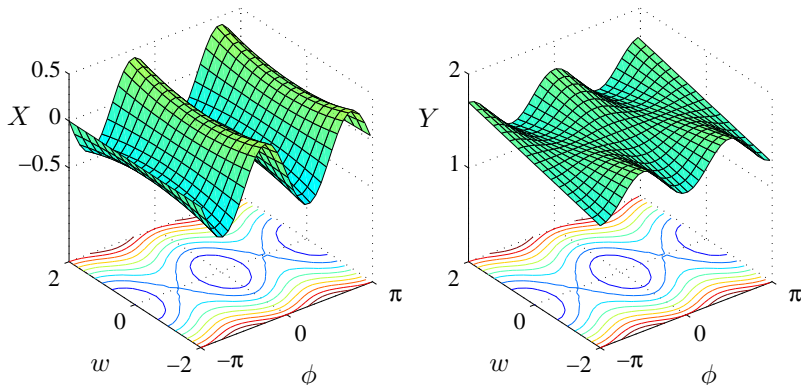


FIG. 2.1. Approximate slow manifold with $O(\epsilon^3)$ accuracy: the slaving functions $X(u, v, w)$ and $Y(u, v, w)$ are plotted as functions of ϕ (with $u = \cos \phi$ and $v = \sin \phi$) and w for $\epsilon = 0.2$ and $b = 0.5$. Approximate slow trajectories are plotted in the (ϕ, w) -plane.

and

$$(2.22) \quad C_{00}^1 = -2b, \quad C_{10}^1 = -b/2, \quad C_{01}^1 = b/2.$$

For larger n , the coefficients are easily computed numerically for fixed b . The numerical results presented in this paper rely on such computations carried out for n up to 100.

The slow manifold corresponding to (2.20)–(2.22), for which the superbalance equation is approximated within an $O(\epsilon^3)$ error, is shown in Figure 2.1. The approximations to X and Y are shown as a function of ϕ and w , with $u_0 = 1$ in (2.6), $\epsilon = 0.2$ and $b = 0.5$. The Figure also shows approximate trajectories in the plane of the slow variables (ϕ, w) ; lifting them to the slow manifold gives an approximation to full trajectories.

The series (2.15) diverge as $N \rightarrow \infty$. In this paper we examine more precisely the nature of this divergence by considering the late behaviour of the slaving coefficients X_n and Y_n as $n \rightarrow \infty$. A possible approach, attempted by Warn [33] for a simplified model, consists in deriving approximations for the polynomial coefficients C_{ij}^n and D_{ij}^n as $n \rightarrow \infty$ from the recurrence relations (2.18)–(2.19). This is carried out in the next section.

3. Late behaviour of C_{ij}^n and D_{ij}^n . We consider the behaviour of C_{ij}^n and D_{ij}^n for large n . Numerical computations of these coefficients suggest the asymptotic forms

$$(3.1) \quad C_{ij}^n \sim (-1)^{j+1} f(\xi, \eta) \quad \text{and} \quad D_{ij}^n \sim (-1)^j g(\xi, \eta),$$

where

$$(3.2) \quad \xi = n^{-1/2}(i - n/3) \quad \text{and} \quad \eta = n^{-1/2}(j - n/3).$$

The two functions $f(\xi, \eta)$ and $g(\xi, \eta)$ introduced in (3.1) are smooth and localized, peaking at $(\xi, \eta) = (0, 0)$ and decreasing rapidly for $|\xi| \rightarrow \infty$ and $|\eta| \rightarrow \infty$. Thus, the

coefficients C_{ij}^n and D_{ij}^n are maximum for $i \approx n/3$ and $j \approx n/3$, and $O(1)$ only in a ‘core’ region where $\xi, \eta = O(1)$. As we now show, it is not difficult to derive explicit expressions for $f(\xi, \eta)$ and $g(\xi, \eta)$ in this core region.

3.1. Core: $\xi, \eta = O(1)$. We first note that the nonlinear terms in the recurrence relations (2.18)–(2.19) (the last two lines in each of these equations) can be neglected in the limit $n \rightarrow \infty$; provided that C_{ij}^n and D_{ij}^n remain $O(1)$ as $n \rightarrow \infty$ this is a valid approximation because of the rapid decrease of the ratios of factorials. Neglecting the nonlinear terms, we obtain two sets of first-order linear recurrence relations and, by elimination of D_{ij}^n , a single set of second-order recurrence relations for C_{ij}^n . Substituting the form (3.1) and using Taylor expansions to write, for instance,

$$\begin{aligned} C_{(i+1)j}^n &\sim (-1)^{j+1} f(\xi + n^{-1/2}, \eta) \\ &\sim (-1)^{j+1} \left[f(\xi, \eta) + n^{-1/2} \frac{\partial f}{\partial \xi}(\xi, \eta) + \frac{1}{2n} \frac{\partial^2 f}{\partial \xi^2}(\xi, \eta) + \dots \right] \end{aligned}$$

leads to a partial-differential equation for $f(\xi, \eta)$. The first non-trivial term appears at order $O(n^{-1})$ and is given by

$$4 \left(\frac{\partial^2 f}{\partial \xi^2} + \frac{\partial^2 f}{\partial \eta^2} - \frac{\partial^2 f}{\partial \xi \partial \eta} \right) + 45 \left(\xi \frac{\partial f}{\partial \xi} + \eta \frac{\partial f}{\partial \eta} \right) + 90f = 0.$$

Separating variables, it is easily verified that the only solution decreasing to 0 for large $|\xi|$ and $|\eta|$ is the Gaussian

$$(3.3) \quad f(\xi, \eta) = \Lambda e^{-15(\xi^2 + \xi\eta + \eta^2)/2},$$

where the constant Λ remains to be determined. From the linearisation of (2.18) and from (3.1), we also deduce that

$$(3.4) \quad g(\xi, \eta) = f(\xi, \eta).$$

With these results, the form of C_{ij}^n and D_{ij}^n for large n is known up to the single number Λ which depends solely on b and needs to be determined numerically. This is conveniently done by considering the behaviour of the solutions $(u(t), v(t), w(t), x(t), y(t))$ of the LK model near their poles in the complex t -plane. This approach makes contact with the exponential-asymptotics treatment of solutions of the LK models in [29].

Let $t_* \in \mathbb{C}$ be one of the poles of the solutions (as discussed below, these are poles of Jacobi elliptic functions but their location is unimportant at this point). At a distance from such a pole, the dependent variables can be expanded in inverse powers of $t - t_*$ as

$$(3.5) \quad u = \sum_{n=0}^{\infty} \frac{\epsilon^{2n} \hat{U}_n}{(t - t_*)^{2n+1}}, \quad v = \sum_{n=0}^{\infty} \frac{\epsilon^{2n} \hat{V}_n}{(t - t_*)^{2n+1}}, \quad w = \sum_{n=0}^{\infty} \frac{\epsilon^{2n} \hat{W}_n}{(t - t_*)^{2n+1}},$$

$$(3.6) \quad x = \sum_{n=0}^{\infty} \frac{\epsilon^{2n} \hat{X}_n}{(t - t_*)^{2n+2}} \quad \text{and} \quad y = \sum_{n=0}^{\infty} \frac{\epsilon^{2n+1} \hat{Y}_n}{(t - t_*)^{2n+3}}.$$

Note that the coefficients \hat{X}_n and \hat{Y}_n are just (complex) numbers, unlike X_n and Y_n which are functions of (u, v, w) . Substituting (3.5)–(3.6) into (2.1)–(2.5) gives a set of 5 first-order recurrence relations for the coefficients $(\hat{U}_n, \hat{V}_n, \hat{W}_n, \hat{X}_n, \hat{Y}_n)$. Observing that

$$(3.7) \quad u \sim -i/(t - t_*), \quad v \sim 1/(t - t_*), \quad w \sim -i/(t - t_*),$$

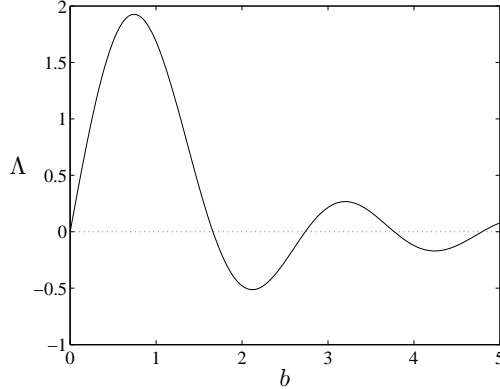


FIG. 3.1. Prefactor Λ in the asymptotics (3.1)–(3.3) of C_{ij}^n as a function of b .

is a possible leading-order behaviour near t_* , we find the initial conditions

$$(3.8) \quad \hat{U}_0 = -i, \quad \hat{V}_0 = 1, \quad \hat{W}_0 = -i, \quad \hat{X}_0 = ib \quad \text{and} \quad \hat{Y}_0 = 2ib$$

for these recurrence relations. There are other possible behaviours near the poles, alternative to (3.7). These are obtained by changing the signs of a pair of (u, v, w) and hence of $(\hat{U}_0, \hat{V}_0, \hat{W}_0)$, and correcting the signs of (\hat{X}_0, \hat{Y}_0) accordingly. (Such an alternative choice is made [29].)

With the initial conditions (3.8) and for fixed b , it is straightforward to compute $(\hat{U}_n, \hat{V}_n, \hat{W}_n, \hat{X}_n, \hat{Y}_n)$ numerically. The value of Λ can then be inferred from their behaviour for $n \gg 1$. Specifically, the late form of \hat{X}_n can be verified to be

$$(3.9) \quad \hat{X}_n \sim i(-1)^n (2n+1)! \kappa,$$

for some constant κ . This constant is easily estimated from the \hat{X}_n obtained numerically by approximating the relation

$$\kappa = \lim_{n \rightarrow \infty} \frac{i(-1)^{n+1} \hat{X}_n}{(2n+1)!}$$

for a large but finite n (cf. [29]).

Now, the asymptotic form (3.1)–(3.3) of C_{ij}^n provides an alternative expression for the right-hand side of (3.9). To obtain it, we substitute the leading-order behaviour of u, v and w near t_* given in (3.7) into the expansion (2.15)–(2.16) of the slaving relation $x = X(u, v, w; \epsilon)$. This reduces to

$$x \sim i \sum_{n=0}^{\infty} \frac{(-1)^{n+1} (2n)! \epsilon^{2n}}{(t-t_*)^{2n+2}} \sum_{i,j=0}^n (-1)^j C_{ij}^n.$$

Comparing with (3.6) then gives

$$\hat{X}_n \sim i(-1)^{n+1} (2n)! \sum_{i,j=0}^n (-1)^j C_{ij}^n.$$

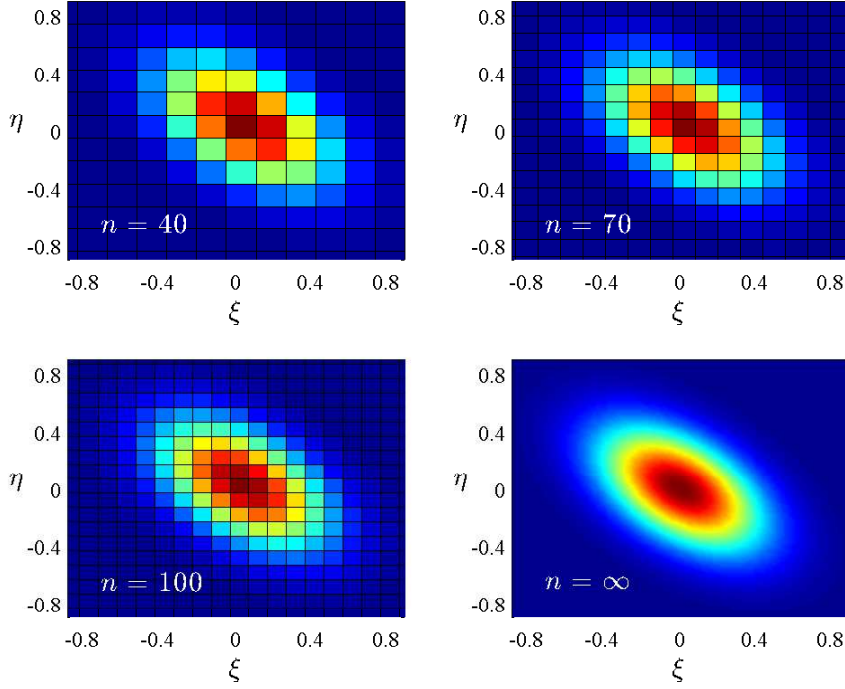


FIG. 3.2. Coefficients $(-1)^{j+1}C_{ij}^n$ as functions of $\xi = n^{-1/2}(i - n/3)$ and $\eta = n^{-1/2}(j - n/3)$ for $n = 40, 70$ and 100 , and for $b = 0.5$. The last panel shows the asymptotic form for $n \rightarrow \infty$.

The right-hand side can now be evaluated using the the form (3.1)–(3.3) of C_{ij}^n . Approximating the sums by integrals, we obtain

$$\begin{aligned} \hat{X}_n &\sim i(-1)^n(2n)!n\Lambda \int_{-\infty}^{\infty} \int_{-\infty}^{\infty} e^{-15(\xi^2+\eta^2+\xi\eta)/2} d\xi d\eta \\ &\sim i(-1)^n(2n+1)! \frac{2\pi\Lambda}{15\sqrt{3}}. \end{aligned}$$

This is a second expression for the late behaviour of \hat{X}_n . Identifying with (3.9) leads to the relation

$$(3.10) \quad \Lambda = \frac{15\sqrt{3}}{2\pi}\kappa.$$

Thus, like κ , Λ can be obtained numerically by computing the coefficients \hat{X}_n for $n \gg 1$ from the five recurrence relations for $(\hat{U}_n, \hat{V}_n, \hat{W}_n, \hat{X}_n, \hat{Y}_n)$. The results of this computation carried out for values of b in the range $(0, 5)$ are shown in Figure 3.1. For the value $b = 0.5$ which we use often in what follows, we find that $\Lambda = 1.6858 \dots$. Note that Λ vanishes for certain values of b ; for these, the growth of the functions X_n and Y_n is slower than in the generic case $\Lambda \neq 0$, and it can only be captured by continuing the expansion beyond the leading-order term considered here.

With our estimate for the prefactor Λ , we now have the complete form of the leading-order asymptotics of C_{ij}^n and D_{ij}^n for $n \gg 1$ in the core region $\xi, \eta = O(1)$.

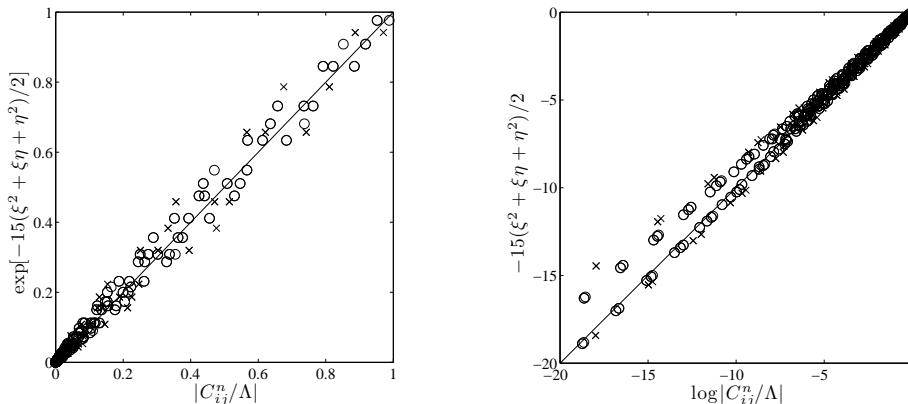


FIG. 3.3. Scatter plot of $(-1)^{j+1}C_{ij}^n/\Lambda$, with Λ estimated numerically, against $\exp[-15(\xi^2 + \xi\eta + \eta^2)/2]$ for $b = 0.5$, and $n = 40$ (\times) and $n = 100$ (\circ). The same data are plotted in linear coordinates (left panel) and in logarithmic coordinates (right panel).

This is compared in figure 3.2 with the values of $(-1)^{j+1}C_{ij}^n$ computed numerically from the recurrence relations (2.16)–(2.19) for $n = 40, 70$ and 100 . The figure confirms the asymptotic results, and illustrates how the discrete dependence of C_{ij}^n on i and j asymptotes to the continuous dependence on ξ and η as $n \rightarrow \infty$. To give a more precise comparison between numerical and asymptotic results than than afforded by the colour-scale figure 3.2, we show in figure 3.3 a scatter plot of $(-1)^{j+1}C_{ij}^n$, normalised by Λ , against its asymptotic limit $\exp[-15(\xi^2 + \xi\eta + \eta^2)/2]$. This confirms the match between asymptotic and numerical results. It also shows that the convergence towards the asymptotic behaviour is rather slow.

A noticeable feature of figure 3.3 is the cloud of points for small values of C_{ij}^n . These correspond to indices i and j far from the core values $i, j \approx n/3$ or, in other words, to $|\xi|, |\eta| \gg 1$. In this tail region, we cannot expect the asymptotics (3.1)–(3.3) to be valid. Even though C_{ij}^n and D_{ij}^n are exponentially small there, the tail region is important for the evaluation of the coefficients X_n and Y_n from the sums (2.16)–(2.17). Indeed, for $u, v, w \in \mathbb{R}$, the largest terms in these sums are not those for which $\xi, \eta = O(1)$ but rather $\xi, \eta = O(n^{1/2})$. This is because the factors $u^{2i+1}v^{2j+1}w^{2k}$ in the sum (2.16), for instance, depend exponentially on n in the core region, since $i, j, k = O(n)$ there. Thus the asymptotic results derived so far, although providing valid estimates for the coefficients C_{ij}^n and D_{ij}^n where they are $O(1)$, are not sufficiently accurate to estimate X_n and Y_n from (2.16)–(2.17).

The situation is analogous to that encountered in probability theory when studying the distribution of the sum of random variables. The central-limit theorem provides a Gaussian approximation for the core of the distribution, but this approximation fails in the tails. These can be essential, however, for instance if the expectation of the exponential of the sum is to be estimated. It is therefore necessary to go beyond the central-limit theorem and use the theory of large deviations, which gives an estimate of the distribution valid in the tails. Here, similarly, it is necessary to derive an approximation for C_{ij}^n and D_{ij}^n for $n \gg 1$ when $\xi, \eta = O(n^{1/2})$. This is done next.

3.2. Tail: $\xi, \eta = O(n^{1/2})$. We start with the ‘large-deviation’ ansatz

$$(3.11) \quad C_{ij}^n = (-1)^{j+1} A(a, b, n) e^{-nG(a,b)},$$

where

$$a = \frac{i}{n} - \frac{1}{3} \quad \text{and} \quad b = \frac{j}{n} - \frac{1}{3}.$$

Here the functions A and G need to be determined to satisfy the recurrence relations (2.18)–(2.19). The dependence of A on n is assumed to be such that its partial derivatives (denoted by subscripts) satisfy $A_a, A_b = O(1)$, as $n \rightarrow \infty$. We will be concerned only with determining the function G which governs the dominant, or controlling, behaviour of C_{ij}^n . This function satisfies

$$G(0, 0) = G_a(0, 0) = G_b(0, 0) = 0.$$

This is necessary to recover the Gaussian form given in (3.1) and (3.3)–(3.4) when $a = n^{-1/2}\xi = O(n^{-1/2})$ and $b = n^{-1/2}\eta = O(n^{-1/2})$. More specifically,

$$(3.12) \quad G(a, b) \sim \frac{15}{2} (a^2 + ab + b^2), \quad \text{as } a, b \rightarrow 0.$$

Introducing (3.11) into (2.18)–(2.19) and retaining only the leading order term yields a nonlinear differential equation for G which is too lengthy to reproduce here. It can however be much simplified by introducing the Legendre transform

$$(3.13) \quad S(p, q) = \sup_{a,b} (ap + bq - G(a, b)),$$

with $p = G_a(a, b)$ and $q = G_b(a, b)$. In terms of S , with p and q as independent variables, the equation satisfied by G takes the form

$$\left[(1 - e^{-p})S_p + (1 - e^{-q})S_q - \frac{1}{3}(1 + e^{-p} + e^{-q}) \right]^2 = e^{S - 2p/3 - 2q/3}.$$

Taking the square root, we obtain

$$(3.14) \quad (1 - e^{-p})S_p + (1 - e^{-q})S_q = \frac{1}{3}(1 + e^{-p} + e^{-q}) - e^{S/2 - p/3 - q/3}.$$

The sign choice is justified by considering this equation for small p and q . Assuming that S is quadratic, (3.14) reduces to

$$pS_p + qS_q + \frac{S}{2} = \frac{1}{9}(p^2 - pq + q^2) + \dots,$$

where \dots denotes cubic and higher-order terms. Solving gives

$$(3.15) \quad S(p, q) \sim \frac{2}{45}(p^2 - pq + q^2) \quad \text{as } p, q \rightarrow 0,$$

which is the Legendre transform of (3.12), as expected.

The nonlinear equation (3.14) can be solved explicitly. Let

$$(3.16) \quad P = \frac{1}{2} \log [(e^p - 1)(e^q - 1)], \quad Q = \frac{1}{2} \log \left(\frac{e^p - 1}{e^q - 1} \right)$$

and

$$(3.17) \quad S(p, q) = \hat{S}(P, Q) + P - \frac{1}{3}(p + q).$$

We note that the branches of the logarithms in (3.16) need to be specified: a suitable choice takes $-\pi/2 < \arg(e^p - 1) \leq 3\pi/2$ and $-3\pi/2 < \arg(e^q - 1) \leq \pi/2$ so that $P(-p, -q) = P(p, q)$ and $Q(-p, -q) = Q(p, q) + i\pi$ for $p, q > 0$. Introducing the variable transformation (3.16)–(3.17) into (3.14) leads to the simpler equation

$$\hat{S}_P = -\frac{e^{(\hat{S}+P)/2}}{[(1 + e^{P+Q})(1 + e^{P-Q})]^{1/2}}$$

involving a P -derivative only. Integrating gives the solution

$$(3.18) \quad \hat{S}(P, Q) = -2 \log \left(\frac{1}{2} \int^P \frac{e^{P'/2}}{[(1 + e^{P'+Q})(1 + e^{P'-Q})]^{1/2}} dP' + C(Q) \right),$$

where the function $C(Q)$ remains to be determined. It can be shown that $C(Q) = 0$ if the lower limit of integration in (3.18) is taken as $-\infty$ so that

$$(3.19) \quad \hat{S}(P, Q) = -2 \log \left(\frac{1}{2} \int_{-\infty}^P \frac{e^{P'/2}}{[(1 + e^{P'+Q})(1 + e^{P'-Q})]^{1/2}} dP' \right).$$

Indeed, this choice ensures that the limiting behaviour (3.15) is recovered for $p, q \rightarrow 0$. To verify this, note that $P \rightarrow -\infty$ and hence $\exp(P) \rightarrow 0$ as $p, q \rightarrow 0$. The denominator of the integrand in (3.19) can then be expanded, leading to

$$\begin{aligned} \hat{S}(P, Q) &= -2 \log \left(\frac{1}{2} \int_{-\infty}^P e^{P'/2} \left[1 - e^{P'} \cosh Q + e^{2P'} \left(\frac{1}{4} + \frac{3}{4} \cosh(2Q) \right) + \dots \right] dP' \right) \\ &= -P + \frac{2}{3} e^P \cosh Q - \frac{2}{5} e^{2P} \left(\frac{1}{4} + \frac{3}{4} \cosh(2Q) \right) + \frac{1}{9} e^{2P} \cosh^2 Q + \dots \end{aligned}$$

On using the approximations $\exp(P+Q) = p + p^2/2 + \dots$, $\exp(P-Q) = q + q^2/2 + \dots$, $\exp(2P) = pq + \dots$ and $\exp(2Q) = p/q + \dots$, this further simplifies into

$$\hat{S}(P, Q) = -P + \frac{1}{3}(p + q) + \frac{2}{45} (p^2 - pq + q^2) + \dots$$

Introducing this result into (3.17) reduces $S(p, q)$ to the form (3.15), as required.

With (3.19) established, the derivation of the large- n behaviour of C_{ij}^n for $\xi, \eta = O(n^{-1/2})$ is complete: $S(p, q)$ can be calculated from (3.17), and the function $G(a, b)$ follows by inverting the Legendre transform (3.13). If the asymptotic form of C_{ij}^n is only used to approximate the coefficients $X_n(u, v, w)$, as is done in the next section, the inversion step is in fact not necessary since the X_n can be expressed directly in terms of $S(p, q)$.

4. Late behaviour of X_n and Y_n . In this section, we present two approaches for the derivation of the asymptotic form of the slaving coefficients X_n and Y_n for $n \gg 1$. One approach relies on our approximation (3.11) for C_{ij}^n ; the other considers the superbalance equation (2.13)–(2.14) directly. We start with the latter approach, which turns out to be somewhat simpler.

4.1. From the superbalance equation. From (2.13)–(2.14), and assuming that the linear terms dominate for large n , we have that

$$(4.1) \quad X_{n+1} \sim - \left(vw \frac{\partial}{\partial u} + uw \frac{\partial}{\partial v} - uv \frac{\partial}{\partial w} \right)^2 X_n,$$

as $n \rightarrow \infty$. This recurrence relation can be solved using characteristics: let $(U, V, W)(t)$ be the solutions of the leading-order slow equations, namely

$$(4.2) \quad \dot{U} = -VW,$$

$$(4.3) \quad \dot{V} = UW,$$

$$(4.4) \quad \dot{W} = -UV,$$

with initial conditions $(U, V, W)(0) = (u, v, w)$. Then the solution of (4.1) can be written as

$$(4.5) \quad X_n(u, v, w) \sim (-1)^n \frac{d^{2n}}{dt^{2n}} \Big|_{t=0} \tilde{X}_0(U(t), V(t), W(t)),$$

Here \tilde{X}_0 is an unknown polynomial, determined by the early iterations when the nonlinear terms neglected in (4.1) are significant. The details of \tilde{X}_0 do not matter: what controls the right-hand side of (4.5) for large n are the singularities of $(U, V, W)(t)$ nearest the origin of the complex t -plane (e.g. [5]). Let t_* and \bar{t}_* , where the overbar denotes complex conjugation, be these singularities, and assume they are poles of order r . These poles should be thought of as functions of the slow variables: $t_* = t_*(u, v, w)$. Then, as $t \rightarrow t_*$,

$$(4.6) \quad \tilde{X}_0 \sim \frac{C}{(t - t_*)^r},$$

where C is a constant which may depend on t_* . The complex conjugate behaviour holds as $t \rightarrow \bar{t}_*$. These behaviours control the late asymptotics of X_n . From (4.5)–(4.6), we obtain this asymptotics in the explicit form

$$X_n \sim \frac{(-1)^n (2n + r - 1)! C}{(r - 1)! (-t_*)^{2n+r}} + \text{c.c.}$$

Comparison with (3.6) and (3.9) then shows that

$$r = 2 \quad \text{and} \quad C = i\kappa,$$

for trajectories $(U(t), V(t), W(t))$ consistent with (3.7). It follows that

$$(4.7) \quad X_n \sim \frac{(-1)^n (2n + 1)! i\kappa}{t_*^{2n+2}} + \text{c.c.}$$

The relationship $t_* = t_*(u, v, w)$ can be made completely explicit using the solution of (4.2)–(4.4). In what follows, we assume that $|w| \geq |u|$. This means that we consider the open trajectories in the (ϕ, w) -plane represented in Figure 2.1. (The case $|w| < |u|$, corresponding to closed trajectories, is treated similarly, by swapping the roles of u and w .) Defining

$$u_0 = \pm \sqrt{u^2 + v^2} \quad \text{and} \quad w_0 = \pm \sqrt{v^2 + w^2},$$

with the signs those of u and w , respectively, the solution of (4.2)–(4.4) can be written in terms of Jacobi elliptic functions as

$$(4.8) \quad U(t) = u_0 \operatorname{cn}(w_0(t - t_0); k),$$

$$(4.9) \quad V(t) = u_0 \operatorname{sn}(w_0(t - t_0); k),$$

$$(4.10) \quad W(t) = w_0 \operatorname{dn}(w_0(t - t_0); k),$$

where the modulus $k = u_0/w_0 \leq 1$ (e.g. [1], Ch. 16). The constant t_0 is determined by the initial conditions $(U, V, W)(0) = (u, v, w)$. With $\phi(u, v)$ defined as in (2.6) and taken in $(-\pi, \pi)$, we find that

$$(4.11) \quad t_0 = -\frac{1}{w_0} F(\phi(u, v); k),$$

where F denotes the elliptic integral of the first kind, defined as

$$F(\phi; k) = \int_0^\phi (1 - k^2 \sin^2 \sigma)^{-1/2} d\sigma.$$

(e.g. [1], Ch. 17).

Now, the poles of the elliptic functions in (4.8)–(4.10) are located on the lattice

$$(4.12) \quad t_* = t_0 + 2r \frac{K(k)}{w_0} + i(2s + 1) \frac{K(k')}{w_0}, \quad r, s \in \mathbb{Z},$$

where $k'^2 = 1 - k^2$ and $K(k) = F(\pi/2; k)$ denotes the complete elliptic integral of the first kind ([1], Ch. 17). The poles nearest the origin clearly have $s = 0$ or $s = -1$. We choose to denote by t_* the pole corresponding to $s = 0$; the pole corresponding to $s = -1$ is its complex conjugate \bar{t}_* . With this convention, the poles nearest the origin are given by t_* and \bar{t}_* , with

$$(4.13) \quad t_* = t_0 + 2r \frac{K(k)}{w_0} + i \frac{K(k')}{w_0}.$$

Here,

$$r = \begin{cases} -1 & \text{for } \phi \in (-\pi, -\pi/2) \\ 0 & \text{for } \phi \in (-\pi/2, \pi/2) \\ 1 & \text{for } \phi \in (\pi/2, \pi) \end{cases},$$

since, according to (4.11), t_0 is a monotonic function of ϕ in $(-\pi, -\pi/2)$, $(-\pi/2, \pi/2)$ and $(\pi/2, \pi)$ which satisfies $t_0 = \mp K(k)/w_0$ for $\phi = \pm\pi/2$ and $t_0 = \mp 2K(k)/w_0$ for $\phi = \pm\pi$. Substituting (4.13) into (4.7) gives the completely explicit form

$$(4.14) \quad X_n \sim \frac{(-1)^n (2n + 1)! i \kappa w_0^{2n}}{(F(\phi(u, v); k) - 2rK(k) - iK(k'))^{2n+2}} + \text{c.c.}$$

for the late asymptotics of X_n . An analogous expression can be derived for Y_n .

Three remarks are in order. The first concerns the sign of the right-hand side of (4.14). Near the pole with $r = 0$, the behaviour of the solution (4.8)–(4.10) is consistent with (3.7), as assumed in the derivation. Near the poles with $r = \pm 1$, the signs of $U(t)$ and $V(t)$ are opposite to those in (3.7), but the sign of X_n remains

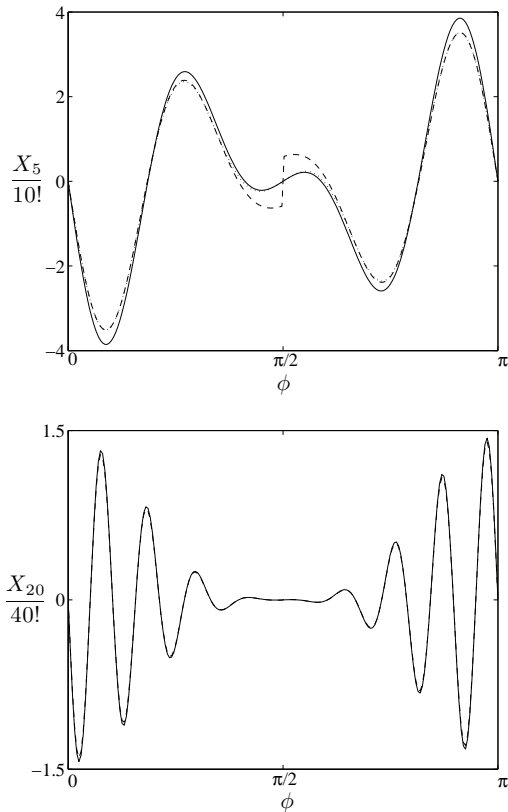


FIG. 4.1. Estimates of $X_n(u, v, w)$ as a function of ϕ for $w = 2$ and $b = 0.5$: numerical results (solid curves) are compared with asymptotic ones (dashed curve) for $n = 5$ and $n = 20$. For $n = 5$ the asymptotic result obtained by taking into two poles is also shown (dotted curve).

unchanged because the transformation $(u, v, w, x, y) \mapsto (-u, -v, w, x, y)$ leaves (2.1)–(2.5) invariant. The second remark concerns the discontinuous behaviour of X_n at $\phi(u, v) = \pm\pi/2$, that is, for $u = 0$. This is immediately remedied by noting that the two pairs of complex-conjugate poles with $r = 0$ and $r = \mp 1$ both contribute to X_n at the same order in a neighbourhood of size $O(n^{-1})$ of $\phi = \pm\pi/2$. Adding the two contributions then leads to an approximation for X_n that is continuous at $\phi = \pm\pi/2$. The third remark is that the factorial growth of X_n described by (4.14) means that the asymptotic series (2.15) defining the slow manifold is of type Gevrey of order 1; the divergence of this type of series and their resummability is well understood (e.g. [2]).

The asymptotic result (4.14) is illustrated by figure 4.1 which compares the asymptotic and numerical estimates of $X_n/(2n)!$ as a function of ϕ for fixed $u_0 = 1$, $w = 2$ and $b = 0.5$. Since X_n is a π -periodic function of ϕ , it is only plotted for $\phi \in [0, \pi)$. The upper panel of the figure corresponds to $n = 5$, and the lower panel to $n = 20$. For $n = 5$, we show two asymptotic estimates: the first takes into account only the pair of complex-conjugate poles nearest the origin; the second takes into account the two nearest pairs. As remarked above, the latter approximation eliminates the discontinuity at $\phi = \pi/2$; it also matches the numerical results remarkably well.

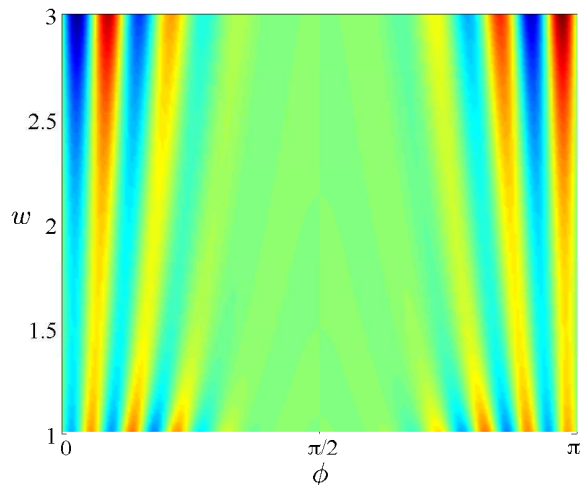


FIG. 4.2. X_{20} as a function of ϕ and w for $u_0 = 1$ and $b = 0.5$. (X_{20} has been normalised by w^{23} for the clarity of the picture.)

For $n = 20$, the match is already excellent with a single pair of complex-conjugate poles, and the curves are indistinguishable.

To illustrate further the manner in which the coefficients X_n depend on ϕ and w , we show in Figure 4.2 results of the numerical computation of X_{20} for $\phi \in [0, \pi)$ and $w \in [1, 3)$. The values of X_{20} increase rapidly with w ; in order to make the dependence on ϕ visible in the colour scale for the smaller values of w , we have plotted X_n/w^α rather than X_n , with the parameter α chosen as $\alpha = 23$ to minimise the variations in colour in the w direction. A completely indistinguishable picture would have been produced had we use the asymptotic estimate for X_{20} in place of the numerical results.

4.2. From the coefficients C_{ij}^n . We now present a derivation of the asymptotics (4.14) alternative to that of the previous section. This relies on the results of section 3 providing the asymptotics of the polynomial coefficients C_{ij}^n with sufficient accuracy that the sums (2.16)–(2.17) can be estimated. A possible advantage of this approach is that it is less tied up to the exact solution of the leading-order balanced model (4.2)–(4.4), and hence to the integrability of that model.

To obtain the asymptotics of X_n from that of C_{ij}^n , we introduce (3.11) into (2.16) to find that

$$(4.15) \quad X_n(u, v, w) \asymp (2n)! \sum_{i,j=0}^n A(a, b) (-1)^{j+1} e^{-nG(a,b)} u^{2i+1} v^{2j+1} w^{2k},$$

with $k = n - i - j$. In this section, we concentrate of the controlling behaviour of X_n for $n \gg 1$ and ignore order-one prefactors. This is indicated by the symbol \asymp . The oscillations introduced by the factor $(-1)^{j+1}$ in the sum make the validity of the expression questionable for $v \in \mathbb{R}$. However, one can use it safely for instance if $\nu = iv \in \mathbb{R}$, then use an analytic continuation argument for $v \in \mathbb{R}$. We proceed in this formal manner. Approximating the sums in (4.15) by integrals over a and b gives

$$(4.16) \quad X_n \asymp (2n)! n^2 (u\nu w)^{2n/3} \int_{-\infty}^{\infty} \int_{-\infty}^{\infty} A(a, b) e^{n[2a \log(u/w) + 2b \log(\nu/w) - G(a,b)]} da db.$$

The integrals can be approximated by Laplace's method to obtain

$$(4.17) \quad X_n \asymp (2n)! n(u\nu w)^{2n/3} e^{S(p,q)},$$

where S is the Legendre transform of G defined in (3.13),

$$p = \log\left(\frac{u}{w}\right)^2 \quad \text{and} \quad q = \log\left(\frac{\nu}{w}\right)^2.$$

Several simplifications occur on using the variable transformation (3.16)–(3.17): this reduces (4.17) to the form

$$(4.18) \quad X_n \asymp (2n+1)! [(w^2 - u^2)(w^2 - \nu^2)]^{n/2} e^{n\hat{S}(P,Q)},$$

where

$$(4.19) \quad P = \frac{1}{2} \log \frac{(w^2 - u^2)(w^2 - \nu^2)}{w^4} \quad \text{and} \quad Q = \frac{1}{2} \log \frac{w^2 - u^2}{w^2 - \nu^2}.$$

At this point, we can re-introduce iv in place of ν and take $v \in \mathbb{R}$. Doing so, we analytically continue the function given by the integral in (4.16) for $v \in i\mathbb{R}$ to $v \in \mathbb{R}$. This provides an approximation to at least one branch of (4.15) thought of as an analytic function of v in the complex plane minus possible branch cuts. Note that the arguments of the logarithm in P and Q are both positive if we assume, as in section 4.1, that $|w| \geq |u|$. However, for our choice of branch for the definition of P and Q , $\arg(e^P - 1) = \arg(u^2/w^2 - 1) = \pi$, $\arg(e^Q - 1) = \arg(-v^2/w^2 - 1) = -\pi$, and hence

$$(4.20) \quad P = \frac{1}{2} \log \frac{(w^2 - u^2)(w^2 + v^2)}{w^4} \quad \text{and} \quad Q = \frac{1}{2} \log \frac{w^2 - u^2}{w^2 + v^2} + i\pi.$$

We now consider the integral appearing in the expression (3.18) for \hat{S} , namely

$$(4.21) \quad I = \int_{-\infty}^P \frac{e^{P'/2}}{[(1 + e^{P'+Q})(1 + e^{P'-Q})]^{1/2}} dP'.$$

and note that the factor $1 + e^{P'-Q}$ in the denominator changes sign in the integration range for $P' = Q - i\pi < P$. We introduce the change integration variable from P' to z' , with

$$z'^2 = \frac{1 + e^{Q-P'}}{1 - e^{2Q}},$$

which maps $P' = -\infty$ to $z' = \infty$, $P' = Q - i\pi$ to $z' = 0$, and $P' = P$ to $z' = z$, where

$$(4.22) \quad z^2 = \frac{1 + e^{Q-P}}{1 - e^{2Q}} = (v/u_0)^2,$$

with the last equality following from (4.20). The change of variables makes it possible to express I in terms of elliptic integrals as

$$\begin{aligned} I &= \left(\int_{Q-i\pi}^P + \int_{-\infty}^{Q-i\pi} \right) \frac{e^{P'/2}}{[(1 + e^{P'+Q})(1 + e^{P'-Q})]^{1/2}} dP' \\ &= -e^{Q/2} [F(\phi(u, v); k) \pm iK'(k)], \end{aligned}$$

where the \pm sign depends on a branch choice and $\phi(u, v) = \sin^{-1}(v/u_0)$ is assumed to be in $(-\pi/2, \pi/2)$. In writing this expression we recover the parameter k appearing in section 4.1 from the computation

$$(4.23) \quad 1 - e^{2Q} = \frac{u^2 + v^2}{v^2 + w^2} = \frac{u_0^2}{w_0^2} = k^2.$$

using (4.20). Similarly, we compute $e^{Q/2} = i(w^2 - u^2)^{1/4}(w^2 + v^2)^{-1/4}$ and finally reduce (4.18) to

$$(4.24) \quad X_n \asymp \frac{(2n+1)!(-1)^n w_0^{2n}}{[F(\phi(u, v); k) \pm iK'(k)]^{2n}},$$

Once the two complex-conjugate contributions are taken into account, this is consistent with (4.14) when $-\pi/2 < \phi < \pi/2$. For $-\pi < \phi < -\pi/2$ and $\pi/2 < \phi < \pi$, other branch choices must be made in (4.21) to recover (4.14).

5. Resummation. Our main aim for examining the late asymptotics of the coefficients X_n and Y_n is to control the divergence of the power-series expansion of the slaving relation (2.12) defining the slow manifold. This makes it possible to ascertain how a unique slow manifold can be defined which, although not invariant, is optimal in a certain sense. A natural way of achieving this is by using Borel resummation. As we now show, the Borel summation [2] of the divergent series (2.15) provides a natural definition of a unique, piecewise-continuous slow manifold, with discontinuities across what might be termed Stokes surface.

We define the Borel transform of $X(u, v, w; \epsilon)$ by the series

$$(5.1) \quad B_X(u, v, w; \xi) = \sum_{n=0}^{\infty} \frac{X_n(u, v, w)}{(2n+1)!} \xi^{2n+1}.$$

The asymptotics (4.7) of X_n ensures that this series converges for $|\xi| < |t_*|$. Analytic continuation can then be used to define B_X for larger $|\xi|$. Formally, X can be recovered from its Borel transform by Laplace transform, according to

$$(5.2) \quad X(u, v, w; \epsilon) = \epsilon^{-2} \int_0^{\infty} e^{-\xi/\epsilon} B_X(u, v, w; \xi) d\xi,$$

as a term-by-term integration indicates. We now propose to define the optimal slow manifold for the LK model by this relation and its counterpart for $Y(u, v, w; \epsilon)$. A crucial point is that we choose the integration contour in (5.2) to be the positive real line for all values of (u, v, w) . A consequence is that the optimal slow manifold defined in this manner is not analytic and indeed not even continuous in (u, v, w) . This is unavoidable since the analytic continuation of (5.2) that may be obtained by suitably deforming the contour of integration in the complex plane picks up fast oscillations across certain surfaces in the (u, v, w) -space. We discuss this next.

The loss of analyticity in X arises when singularities of B_X in the ξ -plane cross the positive real axis. The singularities of B_X are, in turn, controlled by the asymptotics of X_n for $n \gg 1$. Taking (4.7) into account, we observe that B_X has poles for $\xi = \pm it_*$, with the behaviour

$$(5.3) \quad B_X(u, v, w; \xi) \sim \pm \sum_{n=0}^{\infty} (-1)^n i \kappa \frac{\xi^{2n+1}}{t_*^{2n+2}} = \pm \frac{i \kappa \xi}{\xi^2 + t_*^2}$$

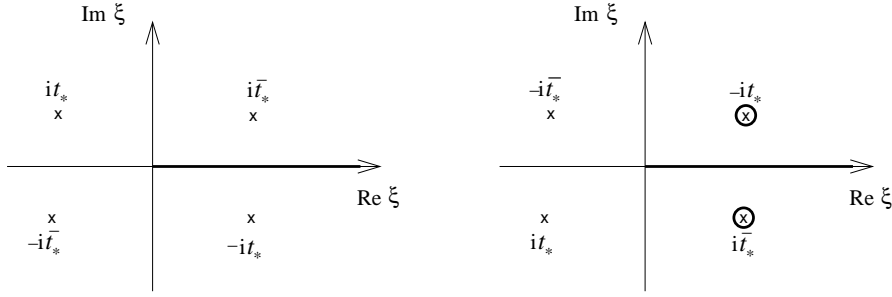


FIG. 5.1. Location of the poles of B_X in the complex ξ -plane for $v < 0$ (left panel), and for $v > 0$ (right panel). The optimal slow manifold, defined by as the integral of $\exp(-\xi/\epsilon)B_X$ along the positive real axis of ξ , is not analytic for $v = 0$: the optimal slow manifold for $v > 0$ differs from the analytic continuation of the manifold defined for $v < 0$ by the contributions of the two poles encircled in the right panel.

near these. Here, as in section 4, t_* is a function of the slow variables: $t_* = t_*(u, v, w)$. The sign should be taken as $+$ if the behaviour of x near the pole is in agreement with (3.7), and as $-$ if the sign of x is opposite. (Note that all poles t_* of $(u(t), v(t), w(t), x(t), y(t))$, not only those nearest the origin, lead to contributions of this form, although the latter have a dominant role.) Thus, we conclude from (5.3) that the optimal slow manifold is discontinuous for values of (u, v, w) such that there are poles t_* with $\text{Re } t_* = 0$. Taking the location (4.12) of the poles t_* into account, this is seen to occur for $\phi = -\pi, 0, \pi$, that is, when $v = 0$. A simple picture therefore emerges of an optimal slow manifold analytic everywhere in (u, v, w) except on the surface $v = 0$, which can be termed Stokes surface. Across this surface, a Stokes phenomenon occurs, and $X(u, v, w; \epsilon)$ and $Y(u, v, w; \epsilon)$ jump. Not surprisingly, the jumps are associated with the generation of fast oscillations.

Let us examine this more closely by considering a trajectory of the slow system crossing the Stokes surface $v = 0$. For definiteness, we consider the crossing corresponding to $\dot{v} > 0$, i.e. $\phi = 0$ (the crossing with $\dot{v} < 0$, i.e. $\phi = \pm\pi$ is the identical modulo a few sign changes). For $v < 0$, the relevant poles of the slow solution (4.8)–(4.10) have $\text{Re } t_* > 0$. Considering only the poles closest to the real axis, and taking $\text{Im } t_* > 0$ by convention, the location of the poles of the function B_X in the ξ -plane (the Borel plane) is as represented on the left panel of Figure 5.1, with four poles at $\pm it_*$ and $\pm i\bar{t}_*$. As v increases toward 0, $\text{Re } t_*$ decreases, and the poles move toward the real line which they cross when $v = 0$. Thereafter, there is a difference between the function X defined by (5.2) for $v > 0$ and the function obtained by analytically continuing X from $v < 0$. The difference is the contribution of the two poles $-it_*$ and $i\bar{t}_*$ that have crossed the integration contour. This contribution, computed from (5.2)–(5.3) (with the $+$ sign) as the residue

$$(5.4) \quad X_{\text{pole}}(u, v, w; \epsilon) = \frac{\pi\kappa}{\epsilon^2} e^{it_*/\epsilon} + \text{c.c.} = \frac{2\pi\kappa}{\epsilon^2} e^{-\text{Im } t_*/\epsilon} \cos(\text{Re } t_*/\epsilon),$$

corresponds to fast gravity oscillations. This is made obvious by evaluating (5.4) along the slow trajectory. To leading order in ϵ , the slow trajectory is given by

$$(5.5) \quad u(t) \sim u_0 \text{cn}(w_0 t; k), \quad v(t) \approx u_0 \text{sn}(w_0 t; k), \quad w(t) \approx w_0 \text{dn}(w_0 t; k).$$

Introducing this into (5.4) leads to

$$(5.6) \quad x_{\text{pole}}(t) = X_{\text{pole}}(u(t), v(t), w(t); \epsilon) = \frac{2\pi k}{\epsilon^2} e^{-K(k')/(\epsilon w_0)} \cos(t/\epsilon),$$

since $-\pi/2 < \phi < \pi/2$, and $t_* = -t + iK(k')/w_0$, in the simple case considered with $\dot{v} > 0$. This pole contribution clearly corresponds to fast oscillations that appear when v goes through 0 and have exponentially small amplitudes, proportional to $\exp(-K(k')/(\epsilon w_0))$. The expression (5.6) coincides with that obtained in [29] using a different approach (up to a sign change arising from a different sign combination in (5.5)). The computations carried out in that paper, comparing (5.6) with results of the numerical integration of the LK system, confirms the validity of this expression.

Physically, the pole contribution represents gravity waves that are generated spontaneously by the slow balanced motion and cause the exact trajectories to move away from the optimal slow manifold by an exponentially small amount. Note that we have considered only the leading-order contribution associated with the pole t_* . In the full problem, there are not only corrections to the amplitude and phase in (5.6), but also terms with higher frequencies n/ϵ , $n > 1$, which appear as a result of the nonlinearities of the LK model.

6. General slow manifold. In this section, we briefly discuss how some of the results obtained above for the LK model generalize to a broad class of two-time-scale systems. The systems that we consider can be written in the form

$$(6.1) \quad \frac{\partial \mathbf{s}}{\partial t} = \mathbf{N}_s(\mathbf{s}, \mathbf{f}),$$

$$(6.2) \quad \frac{\partial \mathbf{f}}{\partial t} + \frac{1}{\epsilon} \mathcal{L}(\mathbf{s})\mathbf{f} = \mathbf{N}_f(\mathbf{s}, \mathbf{f}),$$

where \mathbf{s} denotes the vector of slow variables, and \mathbf{f} the vector of fast variables. Here $\mathbf{N}_s(\mathbf{s}, \mathbf{f})$ and $\mathbf{N}_f(\mathbf{s}, \mathbf{f})$ are vector-valued functions of \mathbf{s} and \mathbf{f} , analytic in finite regions around $\text{Im } \mathbf{s} = 0$ and $\text{Im } \mathbf{f} = 0$. They are assumed to be of order one, and could depend on ϵ , but we have ignored this dependence. The matrix $\mathcal{L}(\mathbf{s})$ governs the linear dynamics of the fast variables; it is assumed to be analytic in \mathbf{s} , and skew symmetric. Its eigenvalues $\pm i\omega_k(\mathbf{s})$, $k = 1, 2, \dots$ of $\mathcal{L}(\mathbf{s})$ are assumed to satisfy

$$1 < \omega_1(\mathbf{s}) < \omega_2(\mathbf{s}) < \dots < \omega_n(\mathbf{s}).$$

The boundedness from below by a constant, which can be set to 1 by suitably defining ϵ , is crucial to ensure the time-scale separation between the variables \mathbf{s} and \mathbf{f} . Note that the fact that $\omega_k \neq 0$ implies that the dimension of \mathbf{f} is even. The LK model is of the form (6.1)–(6.2), with $\mathbf{s} = (u, v, w)$, $\mathbf{f} = \epsilon(x, y)$ and $\mathcal{L}(\mathbf{s})$ given by the 2×2 canonical symplectic matrix.

The system (6.1)–(6.2) clearly has an elliptic slow manifold which, to leading-order, is simply given by $\mathbf{f} = 0$. More accurate slow manifolds can be obtained by seeking a relationship

$$(6.3) \quad \mathbf{f} = \mathbf{F}(\mathbf{s}; \epsilon)$$

slaving the fast variables to the slow ones. Introducing (6.3) into (6.2) and using (6.1) to eliminate the time derivative leads to the superbalance equation

$$(6.4) \quad \epsilon \mathbf{N}_s(\mathbf{s}, \mathbf{F}(\mathbf{s})) \cdot \partial_s \mathbf{F}(\mathbf{s}) + \mathcal{L}(\mathbf{s})\mathbf{F}(\mathbf{s}) = \epsilon \mathbf{N}_f(\mathbf{s}, \mathbf{F}(\mathbf{s})),$$

where \cdot denotes summation over the components of \mathbf{s} . An approximation solution \mathbf{F} can be derived by iteration or expansion in powers of ϵ . Here we use the latter procedure, and write \mathbf{F} as the formal series

$$(6.5) \quad \mathbf{F}(\mathbf{s}; \epsilon) = \sum_{n=0}^{\infty} \epsilon^{n+1} \mathbf{F}^{(n)}(\mathbf{s}).$$

The successive $\mathbf{F}^{(n)}$ are then determined from a recurrence relation, starting with $\mathbf{F}^{(0)}(\mathbf{s}) = \mathcal{L}(\mathbf{s})^{-1} \mathbf{N}_f(\mathbf{s}, 0)$.

6.1. Late behaviour of $\mathbf{F}^{(n)}$. We now consider the asymptotics of $\mathbf{F}^{(n)}$ for $n \gg 1$. In the absence of detailed information on the nature of the terms \mathbf{N}_s and \mathbf{N}_f in (6.1)–(6.2), we cannot write $\mathbf{F}^{(n)}$ as polynomials in \mathbf{s} , as is the case for the LK model (and, more generally, for any model where \mathbf{N}_s and \mathbf{N}_f are polynomials in \mathbf{s} and \mathbf{f}). However, it remains possible to infer the late behaviour of $\mathbf{F}^{(n)}$ directly from the superbalance equation (6.4) following the approach taken for the LK model in section 4.1.

Introducing the expansion (6.5) into (6.4) and considering the coefficient of ϵ^{n+2} , say, leads to a recurrence relation for the $\mathbf{F}^{(n)}$. It would be very tedious to write down this recurrence explicitly; however, our interest is in the behaviour of the solution $\mathbf{F}^{(n)}$ for $n \gg 1$ only. It is therefore sufficient to consider the dominant terms in the recurrence relation; these correspond to the balance

$$(6.6) \quad \mathcal{L}(\mathbf{s}) \mathbf{F}^{(n+1)}(\mathbf{s}) \sim \mathbf{N}_s(\mathbf{s}, 0) \cdot \partial_s \mathbf{F}^{(n)}(\mathbf{s}).$$

To see this, assume that $\mathbf{F}^{(n)}$ depends on n like $(n+r-1)!/a^n$, for some n -independent parameters $r \geq 0$ and $a(\mathbf{s})$, as is confirmed below. The controlling behaviour of the terms retained in (6.6) (i.e., the fastest dependence on n) is then proportional to $(n-r)!$. One of the terms neglected in (6.6) is $\mathbf{F}^{(n)}(\mathbf{s}) \cdot \partial_f \mathbf{N}_f(\mathbf{s}, 0)$, with controlling behaviour $(n+r-1)!$, and hence smaller by a factor $1/n$ than the terms retained. All the other terms are nonlinear in $\mathbf{F}^{(n)}$ and give contributions behaving also like $(n+r-1)!$ or smaller. We demonstrate this for the quadratic terms that arise in the expansion of the first term in (6.4). Ignoring irrelevant constants, these give a contribution at $O(\epsilon^{n+2})$ of the form

$$\sum_{k=0}^{n-1} \mathbf{F}^{(n-1-j)}(\mathbf{s}) \partial_s \mathbf{F}^{(j)}(\mathbf{s}) = \mathbf{F}^{(0)}(\mathbf{s}) \partial_s \mathbf{F}^{(n-1)}(\mathbf{s}) + \sum_{k=0}^{n-2} \mathbf{F}^{(n-1-j)}(\mathbf{s}) \partial_s \mathbf{F}^{(j)}(\mathbf{s}).$$

The first term on the right-hand side behaves like $(n+r-1)!$. The controlling behaviour of each of the terms in the remaining sum can be bounded by $(n+r-2)!$, so that, together, they also yield a contribution bounded by (a multiple of) $(n+r-1)!$. All the nonlinear terms neglected in (6.6) can be treated using a similar argument relying on the fact that multiple sums of powers of $\mathbf{F}^{(j)}$ are dominated by the terms involving the coefficients $\mathbf{F}^{(j)}$ with the largest possible indices j .

Now, the late behaviour of $\mathbf{F}^{(n)}$ can be captured by solving the approximate recurrence relation (6.6). To do this, we define

$$(6.7) \quad \mathbf{v} = \mathbf{N}_s(\mathbf{s}, 0) \cdot \partial_s,$$

which we will think of either as a differential operator or as a vector field in the space of the slow variables \mathbf{s} . The dynamics associated with this vector field is that of the

simplest balanced model, obtained by substituting the lowest-order slaving relation $\mathbf{f} = 0$ into (6.1). The approximate recurrence relation (6.6) can be rewritten in terms of \mathbf{v} as

$$(6.8) \quad \mathcal{L}(\mathbf{s})\mathbf{F}^{(n+1)}(\mathbf{s}) \sim -\mathbf{v}\mathbf{F}^{(n)}(\mathbf{s}).$$

This can be solved using the method of characteristics. We denote by

$$\mathbf{S}(t) = \exp(t\mathbf{v})\mathbf{s}$$

the solution of

$$\dot{\mathbf{S}} = \mathbf{v}(\mathbf{S}) \quad \text{with} \quad \mathbf{S}(0) = \mathbf{s}.$$

Thus $\exp(t\mathbf{v})$ gives the approximate slow trajectory obtained on the leading-order slow manifold $\mathbf{f} = 0$. In terms of this trajectory, we integrate (6.8) as

$$\mathbf{F}^{(n+1)}(\mathbf{s}) \sim -\mathcal{L}(\mathbf{s})^{-1} \left. \frac{d}{dt} \right|_{t=0} \mathbf{F}^{(n)}(e^{t\mathbf{v}}\mathbf{s}).$$

This gives the general solution of (6.6) and hence the leading-order form of the late coefficients as

$$(6.9) \quad \mathbf{F}^{(n)}(\mathbf{s}) \sim (-1)^n \mathcal{L}(\mathbf{s})^{-n} \left. \frac{d^n}{dt^n} \right|_{t=0} \tilde{\mathbf{F}}^{(0)}(e^{t\mathbf{v}}\mathbf{s}; \mathbf{s}),$$

where $\tilde{\mathbf{F}}_0$ is an unknown (vector) function, determined by the early behaviour of the recurrence, when the approximation (6.6) does not hold.

As in the case of the LK model, the large- n behaviour of $\mathbf{F}^{(n)}$ is controlled by the singularities of the function $\psi(t; \mathbf{s}) = \tilde{\mathbf{F}}^{(0)}(e^{t\mathbf{v}}\mathbf{s}; \mathbf{s})$ nearest the origin of the complex t -plane. It is difficult to make general statements about the nature of these singularities, since $e^{t\mathbf{v}}\mathbf{s}$ is the solution of a nonlinear, typically non-integrable system of ordinary differential equations. Poles, branch points, essential singularities, but also more complicated behaviour such as natural boundaries are all possible. Here, we restrict our attention to the simplest situation, where the singularities nearest the real t -axis are a pair of complex-conjugate poles t_* and \bar{t}_* . It should be emphasised that these poles depend on \mathbf{s} , though we do not make this explicit. Near t_* , ψ takes the form

$$(6.10) \quad \psi(t; \mathbf{s}) = \tilde{\mathbf{F}}^{(0)}(e^{t\mathbf{v}}\mathbf{s}; \mathbf{s}) \sim \frac{\mathbf{g}}{(t - t_*)^r},$$

where \mathbf{g} is a time-independent vector, depending on \mathbf{s} only through t_* . In a manner similar to that used to determine κ (or Λ) for the LK model, it should be relatively easy to determine \mathbf{g} by considering solutions of the equations (6.1)–(6.2) in the limit $t \rightarrow t_*$ as expansions in powers of $(t - t_*)^{-1}$.

Introducing (6.10) into (6.9) and taking the complex-conjugate pole into account give

$$(6.11) \quad \mathbf{F}^{(n)}(\mathbf{s}) \sim \frac{(n+r-1)!}{(r-1)!(-t_*)^{n+r}} \mathcal{L}(\mathbf{s})^{-n} \mathbf{g} + \text{c.c.},$$

Now, for generic \mathbf{g} ,

$$(6.12) \quad \mathcal{L}(\mathbf{s})^{-n} \mathbf{g} \sim \frac{\alpha \mathbf{e}_1}{(i\omega_1)^n} + \frac{\beta \bar{\mathbf{e}}_1}{(-i\omega_1)^n}.$$

Here $\pm i\omega_1$ are the lowest eigenvalues of $\mathcal{L}(\mathbf{s})$, \mathbf{e}_1 and its complex conjugate $\bar{\mathbf{e}}_1$ are the associated eigenvectors, normalised so that $\bar{\mathbf{e}}_1 \cdot \mathbf{e}_1 = 1$, where \cdot denotes the (non-Hermitian) scalar product. The constants α and β are given by $\alpha = \bar{\mathbf{e}}_1 \cdot \mathbf{g}$, and $\beta = \mathbf{e}_1 \cdot \mathbf{g}$. Taking (6.12) into account reduces (6.11) to

$$(6.13) \quad \mathbf{F}^{(n)}(\mathbf{s}) \sim \frac{(i)^n (-1)^r (n+r-1)!}{(r-1)! \omega_1^n t_*^{n+r}} (\alpha \mathbf{e}_1 + (-1)^n \beta \bar{\mathbf{e}}_1) + \text{c.c.}$$

In this expression, the dependence on \mathbf{s} of the right-hand side is through that of t_* , α , β , ω_1 and \mathbf{e}_1 . If \mathcal{L} is independent of \mathbf{s} , however, ω_1 and \mathbf{e}_1 are constant, and α and β depend on \mathbf{s} through t_* only. This is the situation of the LK model. Note that (6.13) indicates that the slow manifold is again determined by an asymptotic series of type Gevrey of order 1. Note also that (6.13) has the form $(n+r-1)!/a^n$ assumed to obtain the approximate recurrence relation (6.6).

6.2. Resummation. Once the asymptotic behaviour (6.13) is determined, it is possible to use the Borel summation of the divergent series (6.5) to define a unique optimal slow manifold piecewise. Specifically, we define

$$(6.14) \quad \mathbf{B}_F(\mathbf{s}; \xi) = \sum_{n=0}^{\infty} \frac{\mathbf{F}^{(n)}(\mathbf{s})}{(n+r-1)!} \xi^{n+r-1},$$

which, according to (6.13), converges for $|\xi| < |\omega_1 t_*|$. The formal inversion is given by

$$(6.15) \quad \mathbf{F}(\mathbf{s}; \epsilon) = \frac{1}{\epsilon^r} \int_0^{\infty} e^{-\xi/\epsilon} \mathbf{B}_F(\mathbf{s}; \xi) d\xi,$$

as is readily verified. Like for the LK model, we can choose to define an optimal slow manifold by this expression, insisting that the contour of integration be the positive real line. This slow manifold is discontinuous for the values of \mathbf{s} such that the poles of $\mathbf{B}_F(\mathbf{s}; \xi)$ in ξ lie on the positive real line. The poles of $\mathbf{B}_F(\mathbf{s}; \xi)$ are found from (6.13) to be located at $\pm i t_*$ and $\pm i \bar{t}_*$. Thus the Stokes surfaces, across which the optimal slow manifold is discontinuous, are simply defined by the condition $\text{Re } t_* = 0$.

The analytic continuation of (6.15) across the Stokes surface includes fast oscillations, as we now demonstrate. From (6.13), we obtain that the behaviour of $\mathbf{B}_F(\mathbf{s}; \xi)$ near the poles $\xi = \pm i t_*$ is of the form

$$(6.16) \quad \mathbf{B}_F(\mathbf{s}, \xi) \sim \frac{(-1)^r i \omega_1}{(r-1)!} \left(\frac{\xi}{t_*} \right)^r \left(\frac{\alpha}{\xi + i \omega_1 t_*} \mathbf{e}_1 - \frac{\beta}{\xi - i \omega_1 t_*} \bar{\mathbf{e}}_1 \right).$$

A similar expression gives the behaviour near the complex-conjugate poles $\xi = \pm i \bar{t}_*$. When a Stokes surface is crossed, the difference between the value of \mathbf{F} on the optimal slow manifold and that on the full trajectory is given by the contribution of the poles which cross the positive real axis when $\text{Re } t_* = 0$. Taking $\omega_1 \text{Im } t_* > 0$ for definiteness, these poles are $-i \omega_1 t_*$ and $i \omega_1 \bar{t}_*$. Computing their contribution using the residue theorem gives

$$(6.17) \quad \mathbf{F}_{\text{pole}}(\mathbf{s}; \epsilon) = \pm \frac{2\pi i (i \omega_1)^r}{\epsilon^r (r-1)!} e^{i \omega_1 t_* / \epsilon} \alpha \mathbf{e}_1 + \text{c.c.},$$

where the sign depends on the direction in which $-i t_*$ crosses the positive real axis when $\text{Re } t_* = 0$. Evaluating this expression along the approximate slow solutions

$\mathbf{s}(t) = e^{\mathbf{v}t}\mathbf{s}(0)$ confirms that the pole contribution corresponds to fast oscillations. Their amplitude is the exponentially small $\epsilon^{-r} \exp(-\omega_1 \text{Im } t_*)$, their frequency is the lowest frequency ω_1/ϵ , and their polarisation (relative size of the various components of \mathbf{f}) is fixed by the eigenvector of $\mathcal{L}(s)$ associated with the eigenvalue $i\omega_1$. The other frequencies $\omega_k > 0, k \neq 1$, give contributions that are smaller than (6.17) by the exponentially small factors $\exp[(\omega_1 - \omega_k)\text{Im } t_*/\epsilon]$.

7. Discussion. In this paper, we have examined in detail the divergence of the asymptotic procedures leading to approximately invariant slow manifolds for the Lorenz–Krishnamurthy (LK) model. This divergence was initially observed by Lorenz [20], and considered in some of the subsequent literature [32, 33]. Here we derive an explicit expression for the leading-order behaviour of the slaving coefficients X_n as $n \rightarrow \infty$. This makes it possible to employ Borel summation to define a unique slow manifold. In this manner, we resolve the ambiguity that exists for finite-accuracy slow manifolds which are not uniquely defined even for fixed accuracy ϵ^n . The Borel summation requires to make a choice of integration contour in the Laplace integral that defines it. Our choice is the obvious one which minimizes the oscillations that appear in the slaved fast variables along slow trajectories. The oscillations are not completely eliminated, however: as the trajectories approach the Stokes surface, oscillations appear with the characteristic error-function switching on that characterises the Stokes phenomenon [4]. The definition of the slow manifold that we propose ensures that the oscillations are reduced to sub-exponential levels away from the Stokes surfaces.

We emphasise that our optimal slow manifold differs from Lorenz’s slowest invariant manifold [20]. The latter is a truly invariant manifold consisting of periodic orbits. These periodic orbits exist because the slow system with $\epsilon = 0$ is integrable: its phase space is foliated by periodic orbits most of which persist when $\epsilon \neq 0$ (see [6, 25, 16]). The periodic orbits with $\epsilon \neq 0$ contain exponentially small fast oscillations, with the same amplitude as the oscillations switched on by the Stokes phenomenon that we consider here. In fact it is easy to obtain an approximation for these orbits from our results. This is achieved by adding to a solution which starts on the optimal slow manifold a certain amount of oscillations. The amplitude and phase of these oscillations are chosen such that after a period of the slow solution, when extra oscillations have been switched on by (two) Stokes phenomena, the complete solution returns to its initial value. This is a consistent approximation because, to leading order, the added oscillations are an approximate solution of the LK equations, and because their (exponentially) small amplitudes makes their superposition possible.

We have limited our computations to the leading asymptotics of the slaving coefficients X_n and Y_n for $n \gg 1$. As a result, our estimate for the pole contributions associated with the spontaneous generation of oscillations approximates only the leading-order part of these oscillations. In other words, our computations are carried out to an exponential accuracy that is sufficient to capture the dominant part of the oscillations only. Higher accuracy would require to obtain several terms in the large- n expansion of X_n . A complete expansion for X_n includes terms of different origins. In particular, it includes contributions from all the poles t_* associated with the slow dynamics rather than from those nearest the real axis only. Furthermore, because of the nonlinearity of the recurrence relations for X_n , contributions mixing the different poles arise.

We present two approaches for the determination of the asymptotics of the slaving coefficients. The first, which applies the method of characteristics to the superbalance equation, is readily generalised formally to a large class of two-time scale systems. This

approach makes plain the connection between the exponential asymptotics carried out in [29] for solutions of the LK model and that carried out here for the slow manifold as a whole. In essence, it treats slow manifolds as unions of slow trajectories; in doing so, it turns the problem of exponential asymptotics for the partial-differential equation that is the superbalance equation into a problem of exponential asymptotics for ordinary differential equations. Practical use of this approach requires to compute the location of the poles of the leading-order slow trajectories in the complex time plane. For integrable systems such as the LK model, this is possible very explicitly; however, this can be much more problematic for more complex, non-integrable models. Our second approach relies on the observation that the slaving coefficients X_n and Y_n are polynomials in the slow variables; it concentrates then on first obtaining the asymptotics for the corresponding polynomial coefficients, then summing these. It is clear that the integrability of the LK model underlies the fact that the polynomial coefficients can be obtained in quite an explicit form. It is however possible that this type of approach remains useful in non-integrable problems, provided that the slaving coefficients continue to take polynomial forms. Of course, some numerical work may be required, for instance to evaluate the function G (or its Legendre transform) governing the asymptotics.

We conclude by noting that the control of late coefficients together with Borel summation have been used for two-time-scale systems in the context of averaging [26]. Slow manifolds are of course closely related to averaging, and averaging order by order provides a means of constructing slow manifolds, at least for single-frequency systems, when the difficulties associated with resonances do not arise [15]. In this context, the control of the divergence of asymptotics series can be used as an alternative to the more standard iterative approach, with an incomplete Laplace transform in the Borel summation used in place of the optimal truncation argument to bound error terms by exponentially small quantities. In this paper, we use Borel summation as a practical tool in situations simple enough that the late coefficients in the asymptotic expansions can not only be bounded but also be approximated accurately.

The author thanks J. G. Byatt-Smith, T. N. Bailey, A. M. Davie and A. B. Olde Daalhuis for contributions to this work.

REFERENCES

- [1] M. ABRAMOWITZ AND I. A. STEGUN, *Handbook of mathematical functions*, Dover, 1965.
- [2] W. BALSER, *Formal power series and linear systems of meromorphic ordinary differential equations*, Universitext, Springer-Verlag, New York, 2000.
- [3] C. M. BENDER AND S. A. ORSZAG, *Advanced mathematical methods for scientists and engineers*, Springer, 1999.
- [4] M. V. BERRY, *Uniform asymptotic smoothing of Stokes's discontinuities*, Proc. R. Soc. Lond. A, 422 (1989), pp. 7–21.
- [5] ———, *Universal oscillations of high derivatives*, Proc. R. Soc. Lond. A, 461 (2005), pp. 1735–1751.
- [6] O. BOKHOVE AND T. G. SHEPHERD, *On Hamiltonian balanced dynamics and the slowest invariant manifold*, J. Atmos. Sci., 53 (1996), pp. 276–297.
- [7] J. P. BOYD, *The slow manifold of a five-mode model*, J. Atmos. Sci., 51 (1994), pp. 1057–1064.
- [8] ———, *Eight definitions of the slow manifold: seiches, pseudoseiches, and exponential smallness*, Dyn. Atmos. Oceans, 22 (1995), pp. 49–75.
- [9] R. CAMASSA, *On the geometry of an atmospheric slow manifold*, Physica D, 84 (1995), pp. 357–397.
- [10] R. CAMASSA AND S.-K. TIN, *The global geometry of the slow manifold in the Lorenz–Krishnamurthy model*, J. Atmos. Sci., 53 (1996), pp. 3251–3264.

- [11] C. J. COTTER, *Model reduction for shallow water dynamics: balance, adiabatic invariance and subgrid modelling*, PhD thesis, Imperial College London, 2004.
- [12] C. J. COTTER AND S. REICH, *Semigeostrophic particle motion and exponentially accurate normal forms*, *Multiscale Model. Sim.*, 5 (2006), pp. 476–496.
- [13] N. FENICHEL, *Geometric singular perturbation theory for ordinary differential equations*, *J. Diff. Eq.*, 31 (1979), pp. 53–98.
- [14] A. C. FOWLER AND G. KEMBER, *The Lorenz–Krishnamurthy slow manifold*, *J. Atmos. Sci.*, 53 (1996), pp. 1433–1437.
- [15] V. GELFREICH AND L. LERMAN, *Almost invariant elliptic manifold in a singularly perturbed Hamiltonian system*, *Nonlinearity*, 15 (2002), pp. 447–457.
- [16] ———, *Long periodic orbits and invariant tori in a singularly perturbed Hamiltonian system*, *Physica D*, 176 (2003), pp. 125–146.
- [17] S. J. JACOBS, *Existence of a slow manifold in a model system of equations*, *J. Atmos. Sci.*, 48 (1991), pp. 893–901.
- [18] H. KREISS, *Problems with different time scales for ordinary differential equations*, *SIAM J. Numer. Anal.*, 16 (1979), pp. 980–998.
- [19] H. KREISS AND J. LORENZ, *On the existence of slow manifolds for problems with different time scales*, *Phil. Trans. R. Soc. Lond. A*, 346 (1994), pp. 159–171.
- [20] E. N. LORENZ, *Attractor sets and quasi-geostrophic equilibrium*, *J. Atmos. Sci.*, 37 (1980), pp. 1685–1699.
- [21] ———, *On the existence of a slow manifold*, *J. Atmos. Sci.*, 43 (1986), pp. 1547–1557.
- [22] ———, *The slow manifold — What is it?*, *J. Atmos. Sci.*, 49 (1992), pp. 2449–2451.
- [23] E. N. LORENZ AND V. KRISHNAMURTHY, *On the nonexistence of a slow manifold*, *J. Atmos. Sci.*, 44 (1987), pp. 2940–2950.
- [24] P. LYNCH, *The swinging spring: a simple model for atmospheric balance*, in *Large-scale atmosphere-ocean dynamics*, I. Roulstone and J. Norbury, eds., vol. II: Geometric methods and models, Cambridge University Press, 2002, pp. 64–108.
- [25] R. S. MACKAY, *Slow manifolds*, in *Energy Localisation and Transfer*, T. Dauxois, A. Litvak-Hinenzon, R. S. MacKay, and A. Spanoudaki, eds., World Sci., 2004, pp. 149–192.
- [26] J. RAMIS AND R. SCHÄFKE, *Gevrey separation of fast and slow variables*, *Nonlinearity*, 9 (1996), pp. 353–384.
- [27] R. TEMAM AND D. WIROSOETISNO, *Exponentially accurate approximations for the primitive equations of the ocean*, *Discr. Cont. Dyn. Sys. B*, 7 (2007), pp. 425–440.
- [28] N. G. VAN KAMPEN, *Elimination of fast variables*, *Phys. Rep.*, 124 (1985), pp. 69–160.
- [29] J. VANNESTE, *Inertia-gravity-wave generation by balanced motion: revisiting the Lorenz–Krishnamurthy model*, *J. Atmos. Sci.*, 61 (2004), pp. 224–234.
- [30] ———, *Wave radiation by balanced motion in a simple model*, *SIAM J. Appl. Dynam. Syst.*, 5 (2006), pp. 783–807.
- [31] ———, *Exponential smallness of inertia-gravity-wave generation at small Rossby number*, *J. Atmos. Sci.*, 65 (2008), pp. 1622–1637.
- [32] R. VAUTARD AND B. LEGRAS, *Invariant manifolds, quasi-geostrophy and initialization*, *J. Atmos. Sci.*, 43 (1986), pp. 565–584.
- [33] T. WARN, *Nonlinear balance and quasi-geostrophic sets*, *Atmos.-Ocean*, 35 (1997), pp. 135–145.
- [34] T. WARN, O. BOKHOVE, T. G. SHEPHERD, AND G. K. VALLIS, *Rossby number expansions, slaving principles, and balance dynamics*, *Quart. J. R. Met. Soc.*, 121 (1995), pp. 723–739.
- [35] D. WIROSOETISNO, *Exponentially accurate balance dynamics*, *Adv. Diff. Eq.*, 9 (2004), pp. 177–196.